Molecular Therapy
Original Article

Evaluation of GalNAc-siRNA Conjugate Activity in Pre-clinical Animal Models with Reduced Asialoglycoprotein Receptor Expression

Jennifer L.S. Willoughby,[1,3] Amy Chan,[1,3] Alfica Sehgal,[1] James S. Butler,[1] Jayaprakash K. Nair,[1] Tim Racie,[1] Svetlana Shulga-Morskaya,[1] Tuyen Nguyen,[1] Kun Qian,[1] Kristina Yucius,[1] Klaus Charisse,[1] Theo J.C. van Berkel,[2] Muthiah Manoharan,[1] Kallanthottathil G. Rajeev,[1] Martin A. Maier,[1] Vasant Jadhav,[1] and Tracy S. Zimmermann[1]

[1]Alnylam Pharmaceuticals, Inc., Cambridge, MA 02142, USA; [2]Division of Biopharmaceutics, Leiden Academic Center for Drug Research, 2300 RA Leiden, the Netherlands

The hepatocyte-specific asialoglycoprotein receptor (ASGPR) is an ideal candidate for targeted drug delivery to the liver due to its high capacity for substrate clearance from circulation together with its well-conserved expression and function across species. The development of GalNAc-siRNA conjugates, in which a synthetic triantennary *N*-acetylgalactosamine-based ligand is conjugated to chemically modified siRNA, has enabled efficient, ASGPR-mediated delivery to hepatocytes. To investigate the potential impact of variations in receptor expression on the efficiency of GalNAc-siRNA conjugate delivery, we evaluated the pharmacokinetics and pharmacodynamics of GalNAc-siRNA conjugates in multiple pre-clinical models with reduced receptor expression. Despite greater than 50% reduction in ASGPR levels, GalNAc conjugate activity was retained, suggesting that the remaining receptor capacity was sufficient to mediate efficient uptake of potent GalNAc-siRNAs at pharmacologically relevant dose levels. Collectively, our data support a broad application of the GalNAc-siRNA technology for hepatic targeting, including disease states where ASGPR expression may be reduced.

INTRODUCTION

The hepatic asialoglycoprotein receptor (ASGPR), also known as the Ashwell Morell receptor, is a well-characterized membrane-bound lectin receptor, responsible for removing desialylated glycoproteins from circulation through receptor-mediated endocytosis (RME).[1,2] This hepatocyte-specific receptor is highly expressed and conserved from rodents to human and is comprised of the highly homologous major (ASGPR1) and minor (ASGPR2) subunits. Each subunit consists of a cytosolic *N*-terminal domain, a single transmembrane segment, a stalk domain, and a Ca^{2+}-dependent carbohydrate recognition domain (CRD) at the C terminus.[1,3,4] The CRD is known to mediate binding of non-reducing terminal β-D-galactose or *N*-acetylglactosamine (GalNAc) residues with high affinity.[5,6] Previous reports investigating the ASGPR have shown a receptor recycling time of approximately 10–15 min in human cells,[7,8] a finding consistent with a second dose of GalNAc-siRNA being available for uptake within 10 min of the first dose in rodents.[9] The receptor's ability to facilitate multiple rounds of glycoprotein uptake and clearance, coupled with its ligand specificity, has enabled its use for liver-directed delivery of a wide range of compounds, including small molecules, multi-component systems (e.g., lipid nanoparticles and polymers) and oligonucleotides.[10–16]

We have developed a strategy for targeted delivery of RNAi therapeutics to liver parenchyma based on covalent conjugation of a synthetic trivalent *N*-acetylgalactosamine ligand to chemically modified, metabolically stable siRNA.[9] The GalNAc ligand is designed to bind to the ASGPR with high specificity and affinity, thereby triggering hepatocyte-specific uptake of conjugates, as previously reported using an isolated primary hepatocyte system.[9] This approach has now been validated for a host of RNAi-based therapeutics in pre-clinical models[17–22] and, importantly, has demonstrated successful translation in human clinical trials.[10,12,14] As such, similar targeted delivery strategies have been widely adopted for a variety of nucleic acid therapeutics, including antisense oligonucleotides (ASOs)[13,16] and anti-microRNAs (anti-miRs).[16,23]

To support broad application of the GalNAc conjugate platform, it is essential to advance our understanding of the variables associated with this ligand/receptor system, among them, inter-individual receptor levels and receptor expression in relevant disease settings. ASGPR expression has been clinically correlated to reduced hepatic function in patients diagnosed with liver diseases such as cirrhosis and cancer,[24–28] and reduced receptor expression in rodents has been associated with decrease in clearance of exogenous desialylated glycoproteins.[3,28]

Here, we investigated the impact of reduced ASGPR expression on the pharmacokinetics (PK) and pharmacodynamics (PD) of GalNAc-siRNA conjugates in several reported rodent models with reduced

Received 21 June 2017; accepted 24 August 2017;
https://doi.org/10.1016/j.ymthe.2017.08.019.

[3]These authors contributed equally to this work.

Correspondence: Tracy S. Zimmermann, Alnylam Pharmaceuticals, Inc., Cambridge, MA 02142
E-mail: tzimmermann@alnylam.com

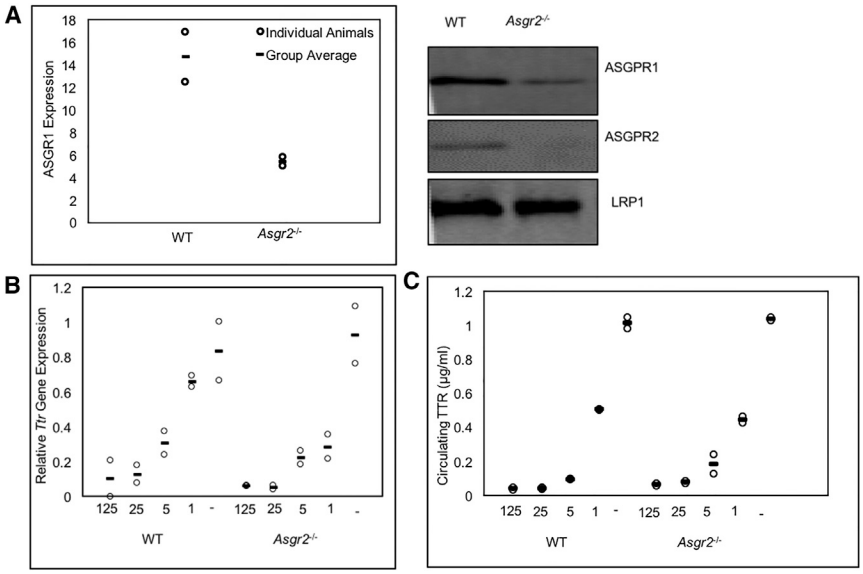

Figure 1. GalNAc-siTTR Retains Potency in *Asgr2*$^{-/-}$ Animals

(A) Membrane-bound ASGPR1 protein expression normalized to an LRP1 loading control was quantified in both WT and *Asgr2*$^{-/-}$ animals (n = 2 animals per group) Representative blot shown (left). (B) *Ttr* gene expression in liver or (C) circulating TTR protein levels were measured after a single subcutaneous dose of GalNAc-siTTR or with a PBS control in either WT mice or *Asgr2*$^{-/-}$ animals. *Ttr* gene expression was normalized to *Gapdh* and is depicted as a percent of the PBS control group (n = 2 animals per group).

ASGPR expression. The first model implements a germline deletion of *Asgr2* in mice that leads to the loss of functional ASGPR2 and destabilization of ASGPR1, thereby yielding reduced but measureable levels of ASGPR1 at the cell surface.[3,29] Two additional pre-clinical models of liver injury, developed in part to be representative of specific human liver pathologies, were also investigated. Specifically, we employed a rodent model of alcoholic liver disease (ALD), whereby reduced binding capacity for ASGPR specific ligands[30] via significant reduction of *Asgr1/2* expression are achieved upon prolonged ethanol (EtOH) exposure.[31] In addition, we also utilized rats treated with the barbiturate, phenobarbital (PB), which has been reported to downregulate ASGPR expression.[32]

The results herein demonstrate that, despite a substantial reduction in ASGPR expression, GalNAc-siRNA conjugate activity is preserved. This is in good agreement with in silico modeling that suggests this high-affinity GalNAc ligand/receptor system has sufficient capacity to maintain adequate uptake and activity of potent GalNAc-siRNA conjugates under simulated conditions of significantly reduced ASGPR levels. Taken together, these data confirm the broad therapeutic potential for targeted oligonucleotide delivery using GalNAc conjugate technology, including hepatic disease settings with potentially reduced receptor expression.[33–35]

RESULTS

GalNAc-siRNA Retains Potency in a Rodent Model with Reduced ASGPR Levels

The impact of reduced functional ASGPR on GalNAc-siRNA conjugate uptake and efficacy was first assessed in the *Asgr2* knockout mouse line (*Asgr2*$^{-/-}$). Detection of membrane-bound ASGPR1 in *Asgr2*$^{-/-}$ mouse livers was found to be approximately 40% of the levels observed in wild-type (WT) animals (Figure 1A), consistent with previous reports.[3,36]

To determine whether the reduction and loss of ASGPR1 and ASGPR2, respectively, resulted in a loss of conjugate potency in vivo, liver *Ttr* transcript and circulating serum TTR levels were assessed in WT and *Asgr2*$^{-/-}$ mice 96 hr post- a single subcutaneous (s.c.) dose of GalNAc-siTTR at 1, 5, 25, or 125 mg/kg (Figures 1B and 1C). Comparable, dose-dependent reductions in *Ttr* mRNA and circulating serum TTR were observed in both *Asgr2*$^{-/-}$ and WT animals.

In order to validate that the retention of GalNAc-siTTR activity observed in *Asgr2*$^{-/-}$ mice was mediated by residual ASGPR1 function, ASGR1 expression was ablated in *Asgr2*$^{-/-}$ mice through an ASGPR-independent delivery mechanism.[37] Animals were dosed intravenously with an *Asgr1*-targeting siRNA or a non-targeting control siRNA formulated in a lipid nanoparticle (LNP-siASGR1 or LNP-siControl, respectively) at a single dose of 1 mg/kg. Loss of residual ASGPR1 expression following LNP-siASGR1 administration was confirmed by western blot (Figures 2A and 2B). Mice dosed with either LNP-siASGR1 or LNP-siControl were then administered a single SC dose of GalNAc-siTTR at 0.2, 1, or 5 mg/kg, previously established to yield ~20%, 50%, and 80% TTR protein suppression, respectively. As expected, dose-dependent serum TTR protein suppression was observed in *Asgr2*$^{-/-}$ animals previously administered with the LNP-siControl. By contrast, animals whose ASGPR1 levels were ablated by pre-treatment with LNP-siASGR1 demonstrated no significant reduction in circulating TTR levels (Figure 2C).

To confirm that GalNAc-siRNA conjugates were specifically targeted to hepatocytes versus other liver cell populations including endothelial and kupffer cells, a ^{125}I radiolabeled GalNAc-siRNA conjugate containing similar chemistry to GalNAc-siTTR2[9] was dosed s.c. at 5 mg/kg in C57BL/6 WT mice. Sixty minutes post-dose, livers were collected, and hepatocytes, endothelial cells, and kupffer cells were isolated to quantify the amount of radiolabeled GalNAc-siRNA conjugate uptake within each cell population. As shown in Figure S1, the GalNAc-siRNA conjugate was overwhelmingly detected in the hepatocyte population consistent with ASGPR-mediated uptake.

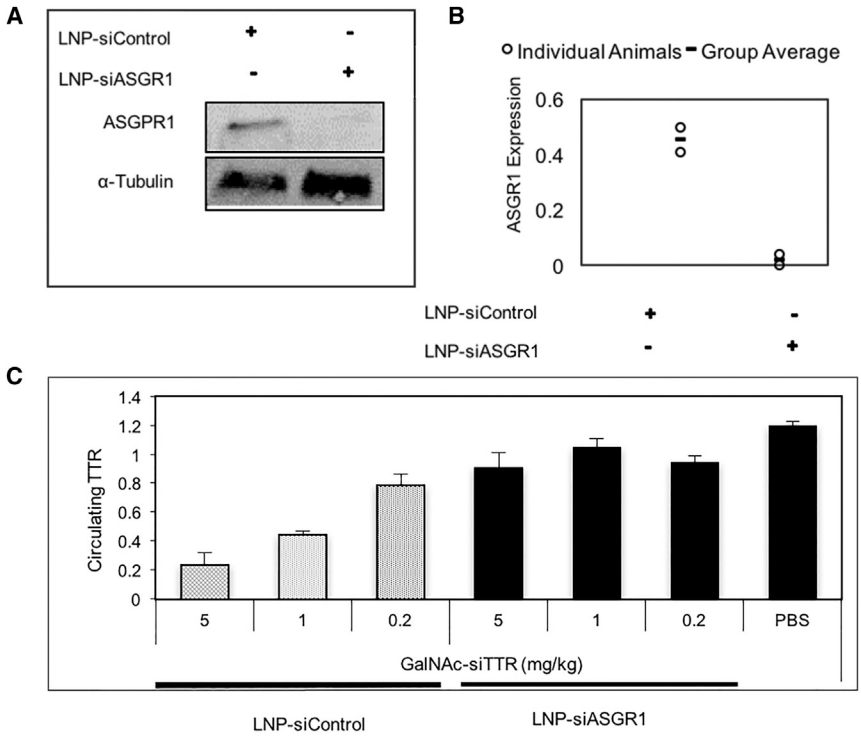

Figure 2. Uptake of GalNAc-siRNA Conjugates Is ASGPR Mediated

Animals were administered a single dose of LNP-siASGR1 or LNP-siControl prior to a single SC dose of GalNAc-siTTR or PBS control. Animals were sacrificed 96 hr post-conjugate-dose for analysis. (A) Western blot and (B) corresponding protein quantitation evaluating ASGR1 expression in livers collected from *Asgr2*$^{-/-}$ animals (n = 2 animals per group). (C) Circulating TTR levels were normalized to each individual animal's pre-dose levels (n = 4 animals per group). Bars are the group average and error bars represent SEM.

Pharmacokinetic Evaluation of GalNAc-siTTR Reveals a Threshold for Receptor-Mediated Uptake in *Asgr2*$^{-/-}$ Mice

To further characterize this model of reduced ASGPR expression and to determine the capacity of the receptor/ligand system in both *Asgr2*$^{-/-}$ and WT mice, plasma, and liver levels of GalNAc-siTTR were quantified after a single SC dose of 1, 5, 25, or 125 mg/kg. At doses of 25 mg/kg and greater, the siRNA concentrations in livers of WT mice were higher than those observed in *Asgr2*$^{-/--}$ animals (Figure 3A). Consistent with the reduction in receptor-mediated liver uptake, plasma siRNA levels in *Asgr2*$^{-/-}$ animals were approximately 2- to 4-fold higher relative to WT animals at 1 hr post-dose (Figure 3B). Collectively, these results indicate that GalNAc-siRNA uptake in *Asgr2*$^{-/-}$ mice is less than dose proportional at dose levels $\geq$25 mg/kg, suggesting that receptor levels are limiting at higher doses.

In an effort to better understand the relationship between ASGPR expression/concentration and hepatic GalNAc-siRNA uptake, an in silico model was developed to evaluate the impact of receptor level on uptake kinetics (Figure 3C). The model incorporates previously described physical properties, including rate constants, receptor/ligand affinities and receptor concentration.[38–43] Simulations were performed at two different siRNA conjugate concentrations, 10 and 500 nM (Figures 3D and 3E), to reflect the approximate maximal plasma concentration, C_{max}, following single administration of approximately 1 and 25 mg/kg GalNAc-siRNA, respectively. In all simulations, binding affinity (K_d), the rate constants of binding and dissociations (k_{on} and k_{off}, respectively), and the ligand internalization rate constant (k_{int}) were held constant (see the legend of Figure 3). In addition to ligand (siRNA conjugate) concentration, the only additional variable parameter was ASGPR concentration. Because the simulations were performed at different concentrations of ligand, the levels of uptake are expressed as fractional values of the total input to allow for comparison. At 10 nM (C_{max} at ~1–2 mg/kg), the model predicts that a reduction of ASGPR from 600 nM to 60 nM has relatively little impact on the fractional rate of conjugate uptake (Figure 3D). By contrast, simulations at 500 nM GalNAc-siRNA (C_{max} at ~25 mg/kg) predict the fractional rate of uptake is much more sensitive to ASGPR concentration (Figure 3E). These simulations are consistent with the in vivo results described above and suggest that changes in receptor concentration alone are sufficient to explain the impact on siRNA PK in liver and plasma in animals with reduced ASGPR levels. Further, the simulations provide a mechanistic explanation for this observation. Even at the lowest ASGPR concentration evaluated (60 nM), the receptor/ligand affinity (K_d ~2 nM) is sufficiently high to promote nearly complete binding at 10 nM ligand concentration (1 mg/kg dose). However, at 500 nM ligand (~25 mg/kg), the receptor concentration becomes limiting, thereby requiring multiple rounds of uptake by the receptor. In this scenario, the rate of uptake depends on the rate of receptor/ligand internalization and receptor recycling.

GalNAc-siRNA Conjugates with Poor Potency Lose Activity in *Asgr2*$^{-/-}$ Settings

The collective in vivo PK and PD results in *Asgr2*$^{-/-}$ mice and in silico modeling data suggested that the capacity of the system in the context of reduced receptor expression becomes rate-limiting at higher doses. Hence, GalNAc-siRNA conjugates with lower potency that require dose levels above 5 mg/kg to reach maximum knockdown would be expected to exhibit reduced in vivo efficacy. To test this hypothesis, we evaluated the activity of two conjugates, GalNAc-siTTR2 and GalNAc-siApoB, with known $ED_{50\text{-}80}$ values of $\geq$25 mg/kg in WT mice owing to early generation chemistry.[9] As seen in Figure 4A, a single 25 mg/kg SC dose of GalNAc-siTTR2

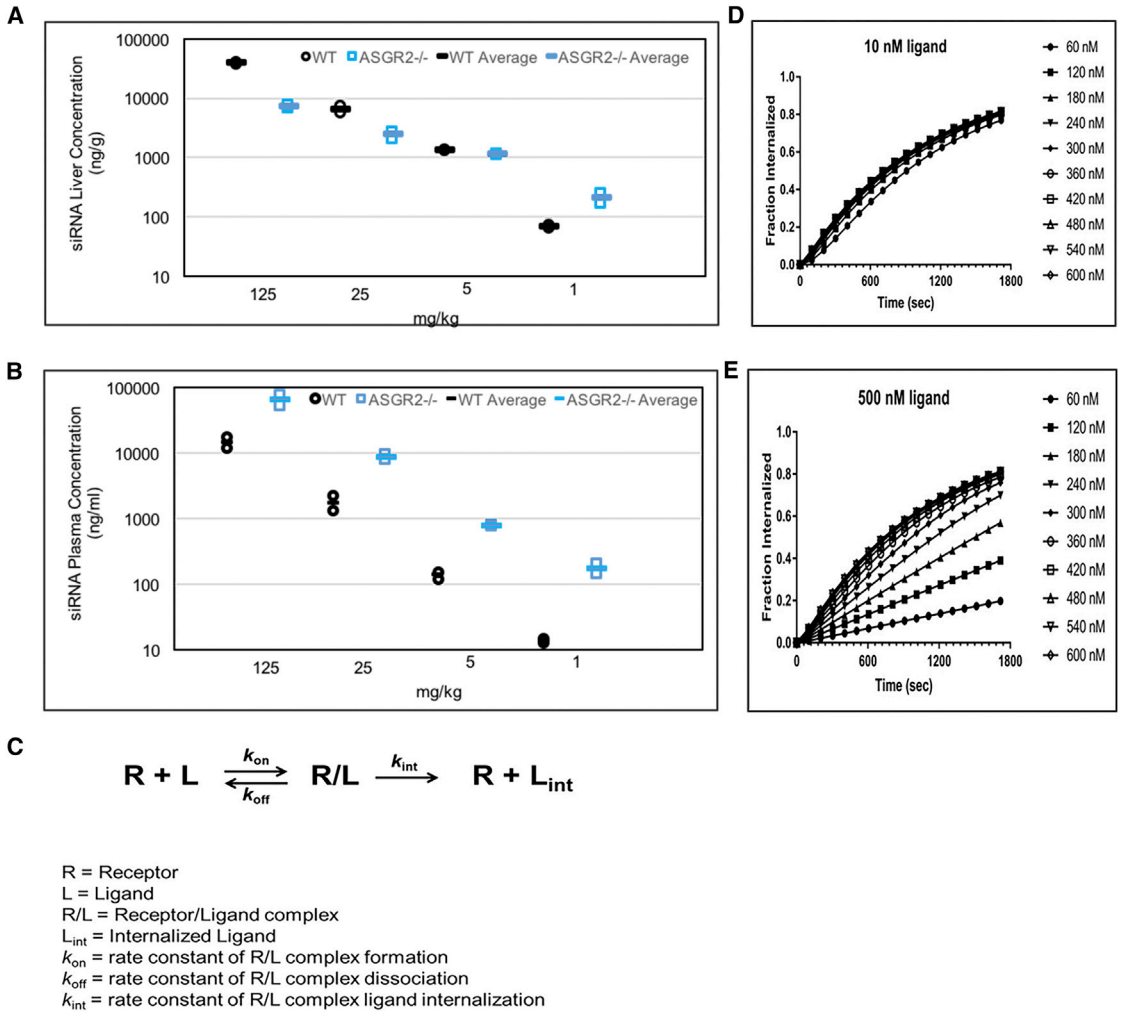

Figure 3. Conjugate Uptake Is Reduced at Dose Levels >5 mg/kg in *Asgr2*$^{-/-}$ Animals

siRNA conjugate concentrations in WT or *Asgr2*$^{-/-}$ animals after a single subcutaneous dose of GalNAc-siTTR or PBS control. siRNA levels were determined using stem loop qPCR in (A) liver collected 96 hr post-dose or (B) 1 hr post-dose detected in plasma (n = 2 animals per group). Liver siRNA concentration is depicted as nanogram per gram (ng/g) of liver. Circulating siRNA is depicted as nanogram per milliliter (ng/mL) of plasma. (C) Schematic of the receptor/ligand binding and internalization model used to evaluate the impact of receptor concentration on hepatic uptake of GalNAc-siRNA. Bars are the group average, and error bars represent SEM. (D and E) Simulated data from the receptor/ligand model predicting the fraction of total GalNAc-siRNA internalized by hepatocytes over time at varying levels of ASGPR concentration when administered at 1 mg/kg (D) or 25 mg/kg (E). Assumptions: K_d = 2 nM; $k_{on} = 1 \times 10^5\ M^{-1}{*}s^{-1}$; $k_{off} = 2 \times 10^{-4}\ s^{-1}$; $k_{int} = 1 \times 10^{-3}\ s^{-1}$; C_{max} (1 mg/kg) = 10 nM; C_{max} (25 mg/kg) = 500 nM; WT ASGPR concentration = 600 nM.[38–43] Plasma concentrations somewhat differ for certain molecules, however, the estimates are that 10 and 500 nM were ~1–2 and ~25 mg/kg.

(ED_{80}) in *Asgr2*$^{-/-}$ animals demonstrated reduced activity as compared to WT at the same time point. Similarly, GalNAc-siApoB dosed at 75 mg/kg (ED_{50}) in WT mice resulted in no measurable target knockdown in the *Asgr2*$^{-/-}$ animals at this dose level (Figure 4B).

GalNAc-siRNA Conjugates Retain Activity in Pre-clinical Liver Injury Models with Reduced Levels of Both ASGPR Subunits

To investigate the impact of more clinically relevant disease states on GalNAc-siRNA activity, two rodent models that recapitulate impaired ASGPR expression were identified, including an EtOH-induced mouse liver injury (Lieber-DeCarli) model[30,31] and a chemically induced PB rat liver injury model.[32]

WT mice that were provided a liquid EtOH diet (36% of total caloric intake) ad libitum for 7 weeks demonstrated an approximately 2-fold reduction of each *Asgr* transcript relative to mice provided a liquid control diet (Figure 5A), consistent with previously published results.[30] To evaluate the impact of GalNAc-siRNA activity under these conditions, a single SC dose of GalNAc-siTTR at 2.5 mg/kg was

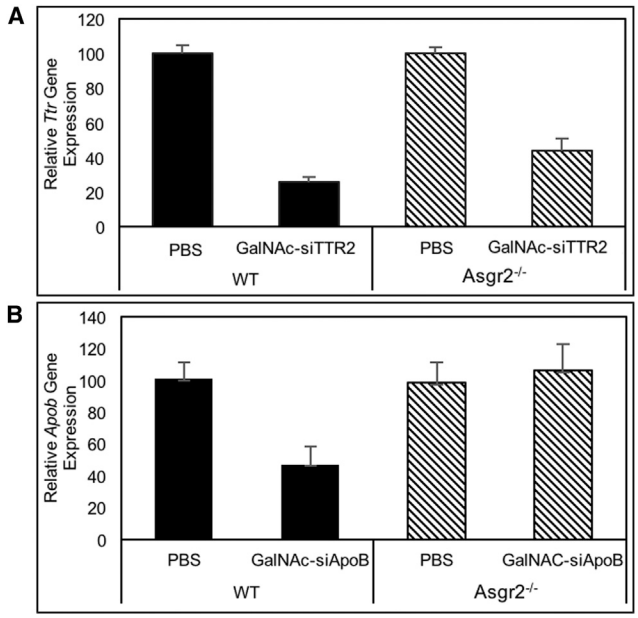

Figure 4. GalNAc-siRNA Molecules with Poor Potency Show Reduced Activity in the *Asgr2*$^{-/-}$ Animals

C57BL/6 or *Asgr2*$^{-/-}$ mice were dosed with a single subcutaneous dose. Relative hepatic gene expression was measured 48 hr post-dose. (A) Animals received a 25 mg/kg dose of GalNAc-siTTR2 or PBS control. Hepatic *Ttr* gene expression was normalized to *Gapdh* and is depicted as a percent of the PBS control group for each animal strain (n = 4 for each group). (B) Animals received a 75 mg/kg dose of GalNAc-siApoB or PBS control. Hepatic *Apob* gene expression was normalized to *Gapdh* and is depicted as a percent of the PBS control group for each animal strain (n = 5 per group). Bars are the group average, and error bars represent SEM.

administered, and TTR mRNA levels were quantified. Activity of the GalNAc-siTTR conjugate was retained in liquid EtOH-fed mice despite a 50% reduction in *Asgr1* and *Asgr2* mRNA expression (Figure 5A).

Comparable results were observed in a second model of liver injury. A 30%–40% reduction in *Asgr1* and *Asgr2* transcript levels was observed in rats induced with four daily IP injections of the hepatic carcinogen, PB, findings consistent with the published data.[32] Equivalent levels of target knockdown were observed 96 hr after a single SC dose of GalNAc-siTTR at 2.5 mg/kg in the absence or presence of PB induction (Figure 5B).

Conjugate Potency Is Retained in a Pre-clinical Model of Liver Fibrosis

Although ASGPR levels have been examined in advanced liver disease states such as cirrhosis and liver cancer, evaluation of fibrotic livers where liver architecture is altered has not yet been assessed. To this point, we examined the ASGPR levels in human and mouse fibrotic liver samples and evaluated conjugate activity in a pre-clinical model of Alpha-1 antitrypsin associated liver disease (AATD). Alpha-1 antitrypsin (AAT) is an abundant plasma protein primarily synthesized and secreted by hepatocytes. The most common mutation causing AAT deficiency, Z-AAT, results in mis-folding, polymerization, and accumulation of AAT protein in hepatocytes, causing a fibro-inflammatory liver disease. This fibro-inflammatory disease results in liver fibrosis that can ultimately advance to liver cirrhosis and hepatocellular carcinoma.[44,45] AATD patients and transgenic (Tg-PiZ) mouse livers expressing the human Z-AAT were compared to normal healthy humans and mice, respectively (Figures 6A and 6B). ASGPR expression levels as assessed by immunohistochemical staining were similar in hepatocytes, even in areas next to fibrotic zones (Figure 6A). As expected, the Tg-PiZ mice also showed an increase in fibrotic markers like collagen1a1 (*Col1a1*) when compared to WT controls (Figure 6C). Despite the presence of fibrotic tissue (Figures 6A–6C), conjugate activity was retained in Tg-PiZ animals as monitored by RNAi activity of GalNAc-TTR siRNA. These data indicate that in fibrotic livers, GalNAc-siRNA conjugates can be taken up by hepatocytes and elicit the desired target gene knockdown effect (Figure 6D).

DISCUSSION

Hepatocyte-specific delivery of therapeutics for the treatment of liver-expressed disease targets has been enabled by recent advances in the GalNAc conjugate platform, supporting the clinical development of several nucleic acid-based therapeutics, including GalNAc-siRNAs.[11,12,14,15,22,46,47] In this report, we investigate the performance of a GalNAc-siRNA conjugate across several pre-clinical models of compromised ASGPR expression.

Deletion of *Asgr2*$^{-/-}$ in mice has been reported to result in loss of functional ASGR2, as well as a destabilization of ASGR1 that leads to reduced (40% of WT) levels of ASGR1 at the cell surface.[3] Despite this diminished receptor expression, potent GalNAc-siRNA conjugates retained efficacy in this model. To confirm that the observed activity was mediated by residual ASGPR1, we utilized LNP-delivered siRNA to effectively silence *Asgr1*. Ablation of ASGR1 expression in the context of *Asgr2*$^{-/-}$ animals resulted in a complete loss in GalNAc-siRNA activity. These data confirm that GalNAc-siTTR liver uptake was specifically mediated through the ASGPR, with subunit ASGR1 being critical for efficient conjugate delivery.

Evaluation of GalNAc-siRNA PK in *Asgr2*$^{-/-}$ mice demonstrate receptor saturation at dose levels >5 mg/kg, as evidenced by an increase of circulating GalNAc-siTTR plasma levels and lower liver levels relative to WT animals. These data suggest that despite severely compromised receptor expression in ASGR2 null mice, residual ASGR1 receptor capacity is not limiting for efficient uptake of conjugates at pharmacologically relevant doses ($\leq$5 mg/kg). However, at dose levels greater than 5 mg/kg, the efficiency of conjugate uptake in hepatocytes of *Asgr2*$^{-/-}$ animals decreases due to receptor saturation. An in silico model of receptor/ligand binding and uptake reproduces this observation and suggests that reduced ASGPR expression, as the lone variable is sufficient to account for this effect. Further, the model provides a mechanistic explanation for this finding. In short, given the relatively high affinity for the GalNAc ligand, ASGPR retains the

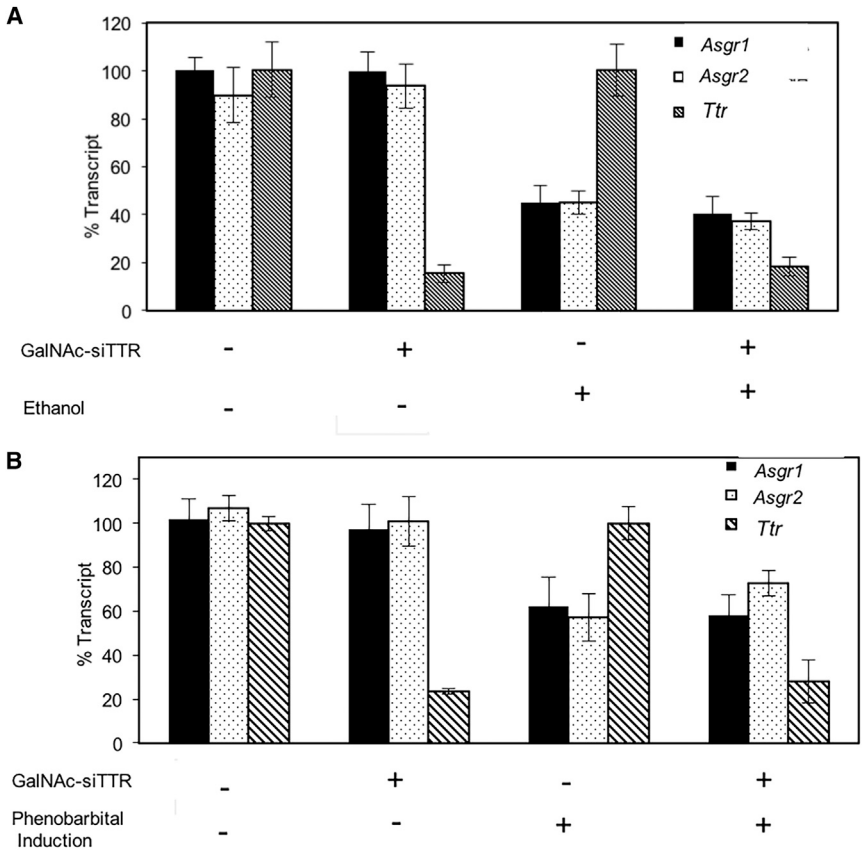

Figure 5. Retention of siRNA-GalNAc Conjugate Activity in Liver Disease Models

(A) C57BL/6 mice were provided Lieber-DeCarli oral liquid diet or control liquid diet ad libitum. Mice on either diet received a single SC dose of GalNAc-siTTR. Animals were sacrificed 96 hr post-dose; *Asgr1*, *Asgr2*, and *Ttr* liver mRNA levels were normalized to a ubiquitous control gene, *Gapdh*. *Asgr1* and *Asgr2* values are depicted as a percent of PBS-treated animals fed control diet, whereas percent TTR levels are depicted as percent of PBS control on Lieber-DeCarli diet (n = 3 per group). (B) Retention of GalNAc-siTTR conjugate activity in phenobarbital-induced liver injury model. Sprague-Dawley rats treated with or without phenobarbital received a single subcutaneous dose of GalNAc-siTTR. Animals were sacrificed 96 hr post-dose where gene expression of *Asgr1*, *Asgr2*, and *Ttr* in rat liver was determined using qPCR. *Asgr1*, *Asgr2*, and *Ttr* gene expression normalized to a ubiquitous control gene, *Gapdh* (n = 3 per group). *Asgr1* and *Asgr2* levels are depicted as a percentage of the non-phenobarbital-treated animals, and *Ttr* levels are depicted as a percentage of the PBS control animals with phenobarbital treatment. Bars are the group average, and error bars represent SEM.

capacity to efficiently bind and internalize GalNAc-siRNA, provided GalNAc-siRNA concentration is less than ASGPR receptor concentration. This would suggest that full therapeutic activity will be retained in a setting of reduced ASGPR expression, provided the required therapeutic dose levels remain below this ASGPR concentration "threshold" limit. This is further supported by the evaluation of two low-potency GalNAc-siRNA molecules that demonstrated either a reduction or complete loss of target silencing in *Asgr2*$^{-/-}$ animals. To this end, it is vital to maximize intrinsic potency of the siRNA to collectively reduce hepatic exposure and subsequent dose level required for therapeutic efficacy.

Evidence of reduced ASGPR in human subjects, as assessed by either immunohistochemistry of liver biopsies or an increase in serum glycoproteins, have been reported in certain disease settings, including congestive heart failure, alcoholic cirrhosis, Laennec's cirrhosis, biliary cirrhosis, as well as in patients with hepatic neoplasms and hepatocellular carcinoma.[24,28,33] Here, we evaluated whether reduced receptor levels have a consequence on GalNAc-siRNA activity using pre-clinical disease models that represent the potential clinical experience of variable receptor expression. Data generated in two pre-clinical liver disease models (EtOH and PB-induced receptor reduction)[32,48] demonstrated full retention of GalNAc-siTTR conjugate activity despite 30%–50% receptor reduction, indicating the potential application of GalNAc-siRNA even in disease settings that may have lower receptor levels.

Additional characterization of ASGPR expression in diseases with liver pathology is essential as we continue to investigate the broad application and development of the ASGPR-mediated drug delivery platform. To this end, we assessed ASGPR levels in fibrotic liver samples from AAT-PiZZ patients and a Tg-PiZ fibrotic mouse model. PiZZ patients with AATD develop liver fibrosis, as shown by an increase in hepatic fibrotic areas or with an increase in mRNA levels for fibrotic markers like *Col1a1*.[49] ASGPR levels were found to be similar to normal healthy livers, even in livers that showed severe fibrosis. Further, retention of conjugate efficacy was observed in the Tg-PiZ model even in the presence of altered liver architecture. These results suggest that potent GalNAc-conjugated siRNAs should be functional in the context of AAT-PiZZ fibrotic livers.

In summary, we demonstrate in a number of genetically and chemically induced pre-clinical models of compromised receptor expression that conjugate potency is both receptor specific and robust. Importantly, the collective data highlight the need for continued development of highly potent GalNAc conjugates, specifically those with therapeutic dose levels that fall below saturation of available ASGPR capacity. Together, these data provide mechanistic insight and guidance for the continued development of GalNAc-siRNA technology and support its broad clinical application for hepatic targeting, including disease states where receptor expression may be compromised.

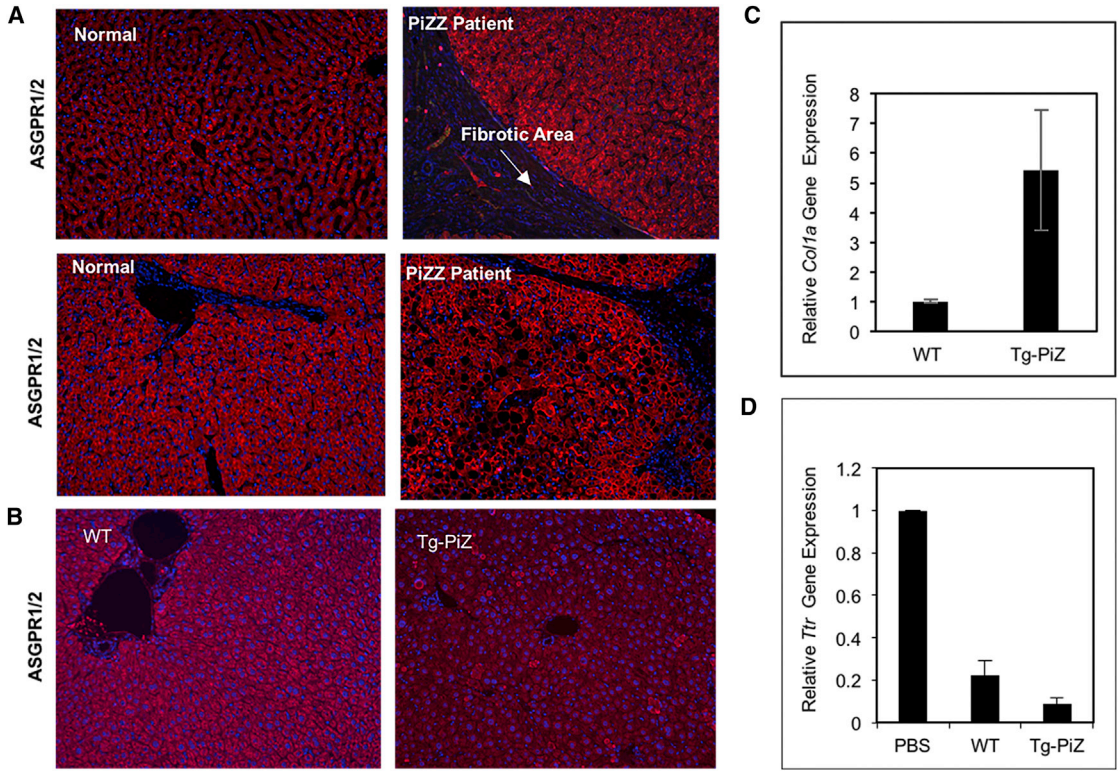

Figure 6. ASGPR Activity Is Retained in a Fibrotic Model

(A) Immunohistochemical staining of liver sections from normal or PiZZ patients. Red, ASGPR1/2 staining; blue, DAPI staining for nucleus. (B) ASGPR levels in Tg-PiZ mice as detected by immunohistochemical staining. Red, ASGPR1/2 staining; blue, DAPI staining for nucleus. (C) mRNA levels of fibrotic marker collagen1a1 (*Col1a1*), normalized to housekeeping gene *Gapdh* in mouse livers. (D) *Ttr* levels after 1.5 mg/kg single dose of GalNAc-siTTR in WT and Tg-PiZ mice (n = 3–5). Bars are the group average, and error bars represent the SD.

MATERIALS AND METHODS

siRNA Synthesis

All oligonucleotides were prepared as described in Nair et al.[9]

Animal Studies

All procedures using mice were conducted by certified laboratory personnel using protocols consistent with local, state, and federal regulations. Experimental protocols were approved by the Institutional Animal Care and Use Committee (IACUC), the Association for Assessment and Accreditation of Laboratory Animal Care International (accreditation number: 001345), and the Office of Laboratory Animal Welfare (accreditation number: A4517-01). All WT control animals were randomly assigned to cages upon facility arrival. For each study, control animals were selected to age and gender match those selected from the colonies of the *Asgr2*$^{-/-}$ or Tg-Piz colonies or those with induced liver injury. When deciding on sample numbers for animal studies, we determined the final number required to be one that would allow for confidence in the resulting dataset utilizing the least number of animals, as required in accordance with IACUC guidelines. *Asgr2*$^{-/-}$ animals from the in-house colony were chosen based on age ranging from 6 to 12 weeks and randomly assigned to each group. WT C57BL/6 or *Asgr2*$^{-/-}$ animals were dosed s.c. with GalNAc-siTTR at doses of 1, 5, 25, or 125 mg/kg or PBS control for the studies described, with animals being sacrificed 96 hr post-dose. Additionally, *Asgr2*$^{-/-}$ animals were dosed intravenously with LNP-siASGR1 or LNP-siControl based on body weight with animals receiving 10 μL per gram. Eleven days following the LNP-siRNA injections, the animals were dosed s.c. with 1, 2.5, or 5 mg/kg of GalNAc-siTTR or PBS control. Finally, *Asgr2*$^{-/-}$ or WT C57BL/6 control animals were dosed with PBS control, GalNAc-siTTR2 at 25 mg/kg, or GalNAc-siApoB at 75 mg/kg. Animals were scarified 48 hr after the final dose. Tg-PiZ mice were obtained from St. Louis University. Tg-PiZ mice received a single, s.c. dose of 1.5 mg/kg of GalNAc-siTTR.

Pharmacokinetic Analysis

C57BL/6 female mice, aged 6–8 weeks, acquired from Charles River Laboratories, were administered GalNAc-siTTR conjugates s.c. with a volume of 10 μL per gram of body weight at dose levels of 1, 5, 25, or 125 mg/kg. Animals from each study group were sacrificed at desired time points to harvest plasma and liver samples for analysis.

Mice were perfused with saline following blood collection and prior to organ harvest. GalNAc-siTTR plasma and liver levels were quantified via stem loop RT-qPCR. In short, aliquots of liver tissue (frozen, powdered) were reconstituted to 100 mg/mL or plasma diluted 10-fold in PBS with 0.25% Triton X-100 and lysed by boiling. The resulting supernatant subsequently was utilized to generate antisense specific cDNA using a sequence-specific stem loop cDNA primer. Antisense strand levels were read using a sequence-specific Taqman assay and a Light cycler 480 system (Roche). siRNA concentration was determined by extrapolation from the standard curves generated by spiking the various concentrations of the synthetic siRNAs into the naive tissue and processed as described above. The lower limit of quantification (LLOQ) for plasma and liver were ~0.005 ng/mL and ~0.1 ng/g, respectively, for siTTR conjugates. Sequence-specific primers used in the stem loop qRT-PCR assay include the following oligonucleotides listed 5′ to 3′: stem loop (GTCGTATCCAGTG CAGGGTCCGAGGTATTCGCACTGGATACGACAAAACA), forward primer (TCGTTATAGAGCAAGAACACT), universal primer (GTGCAGGGTCCGAGGT), and probe ((6-FAM)-CTGGATAC GACAAAACA-(MGB)-(NFQ)).

EtOH-Diet Mouse Model

WT C57BL/6 mice were acquired at 5 weeks of age and were randomized on arrival. Mice were provided Lieber-DeCarli oral liquid diet (5% by volume EtOH = 36% of total calories) or control liquid diet (matched liquid diet composition, 0% EtOH), ad libitum for 5 weeks (maintenance phase). Twenty-four hours post-completion of the maintenance phase, mice received a single s.c. dose of GalNAc-siTTR at 2.5 mg/kg. Animals were sacrificed 96 hr post-dose, and livers were analyzed by qPCR for *Asgr1*, *Asgr2*, and *Ttr* expression.

PB-Induced Liver Injury Model

Four daily intraperitoneal injections of PB were administered to Sprague-Dawley rats (Induction Phase). Twenty-four hours following the final PB administration, rats were dosed a single s.c. dose with either 2.5 mg/kg of GalNAc-siTTR or PBS control. Animals were sacrificed 96 hr post-dose, and livers were analyzed by qPCR for *Asgr1*, *Asgr2*, or *Ttr* expression. Target gene expression was normalized to a ubiquitously expressed housekeeping gene, specifically, *Gapdh*.

Measuring Gene Expression

Gene expression was measured with either a hybridization based assay from Affymetrix as previously described[18] or with RT-qPCR. For RT-qPCR analysis, RNA was isolated from samples using the QIAGEN RNAeasy kit following the manufacturer's instructions. RNA concentrations were determined using a Nanodrop spectrophotometer (Thermo Fisher Scientific). The RNA concentrations were adjusted to 25 ng/μL, where 250 ng RNA was then used to make cDNA using a Reverse Transcription kit from Applied Biosystems (catalog number 4368814). All probes for RNA quantification were acquired from Life Technologies utilizing their Taqman gene expression system. Target gene expression was normalized to the *Gapdh* ubiquitous control in each well utilizing a dual label system. Cp values were measured using a Light Cycler 480 (Roche).

Circulating Serum Transthyretin Levels

Serum samples were diluted 1:4,000 (mouse) and assayed using a commercially available kit (catalog number 41-PALMS-E01) from ALPCO for specific detection of mouse Prealbumin transthyretin as per manufacturer's instructions. Protein concentrations (μg/mL) were determined by using a purified TTR protein standard prepared in-house.

Immunoblotting

Cells were lysed in RIPA buffer (125 mM Tris HCl, 150 mM NaCl, 0.1% NP-40, 1.0% sodium deoxycholate, 1.0% SDS [pH 7.6]) containing ROCHE protease cocktail phosphatase inhibitors (Sigma Aldrich 4693159001) at the manufacturer's recommended concentrations. Lysates were loaded onto 10- or 15-well 4%–20% Mini-PROTEAN TGX Precast gradient gels (Bio-Rad, product number 456-1096). The proteins were transferred to a PVDF membrane using the Bio-Rad wet transfer apparatus for 30 min at 90 V or the iblot system from Invitrogen according to the manufacturer's protocol. PDVF membranes were incubated for 1 hr in odyssey blocking buffer (LI-COR Biosciences cat# 927-40000). The primary antibodies acquired from Abcam, anti-ASGR1 (ab49355) and anti-LRP1 (ab28320), were used at the recommended concentrations. PVDF membranes were then imaged using the Li-Cor Odyssey.[50] Infrared detection quantitated each band on an individual pixel basis using western analysis tools in the Image Studio program.[50]

Membrane Isolation

Livers were snap frozen, ground into powder, and re-suspended in ice-cold homogenization buffer (0.1 M Tris-HCl [pH 7.5], 10 mM EDTA, and 150 mM KCl with Roche complete mini protease inhibitor cocktail) solution. The cells were homogenized on ice with a Fisher Scientific PowerGen Model 125 homogenizer. The cells were centrifuged for 15 min at 12,000 × *g* at 4°C, and the pellet was re-suspended in ice-cold wash buffer (0.1 M Tris-HCl [pH 7.5] with 10 mM EDTA and Roche complete mini-protease inhibitor cocktail), homogenized on ice, and then centrifuged for 45 min at 105,000 × *g*. Finally, the pellet was re-suspended in 3 volumes of microsome buffer (0.05 M Tris-HCl [pH 7.5] with 10 mM EDTA, 20% glycerol, and Roche complete mini-protease inhibitor cocktail). The lysates were homogenized for a final time, aliquoted, flash frozen and stored at −80°C until analysis.

Human PiZZ Samples

Human liver sections from healthy subjects and patients with Alpha-1 antitrypsin deficiency were procured from the National Disease Interchange (NDRI).

Radiolabeled GalNAc-siRNA Studies

A GalNAc-siApoB conjugate was radiolabeled with ^{125}I as previously described in Nair et al.[9], and the cellular distribution studies were executed as previously described.[51]

SUPPLEMENTAL INFORMATION

Supplemental Information includes one figure and can be found with this article online at https://doi.org/10.1016/j.ymthe.2017.08.019.

AUTHOR CONTRIBUTIONS

J.L.S.W., A.C., J.S.B, A.S, J.K.N., M.A.M., V.J., and T.S.Z. drove the research conceptualization and design and analyzed the data. K.C. provided materials. J.L.S.W designed and generated the studies executed in the *Asgr2*$^{-/-}$ animals. M.Y. executed the in vivo portion of the pharmacokinetic evaluation with S.S.-M. and T.N. developing and executing the pharmacokinetic analysis. J.S.B. generated the in silico modeling data with insight from J.K.N. based on binding studies executed by K.Y. A.C. identified liver injury models, EtOH, and phenobarbital, and designed the studies. A.S. led the investigations in the fibrotic model with K.Q. generating the expression and knockdown data. T.R. generated in vivo data for all liver injury models. T.J.C.v.B. radiolabeled the GalNAc-siRNA conjugate and generated the data evaluating cellular distribution in liver. J.L.S.W., A.C., and T.S.Z. wrote the manuscript with key input from A.S., J.S.B., J.K.N., V.J., and M.A.M.

CONFLICTS OF INTEREST

The authors declare competing financial interests: all authors are employees or collaborators of Alnylam Pharmaceuticals.

ACKNOWLEDGMENTS

We thank the Alnylam chemistry and analytical group for providing siRNAs. Special thanks to Madeline Youniss, Jessica Newton, and Matthew Algarin for study support. Thanks for critical input from Kevin Fitzgerald and Rachel Meyers.

REFERENCES

1. Grewal, P.K. (2010). The Ashwell-Morell receptor. Methods Enzymol. *479*, 223–241.
2. Pricer, W.E., Jr., Hudgin, R.L., Ashwell, G., Stockert, R.J., and Morell, A.G. (1974). A membrane receptor protein for asialoglycoproteins. Methods Enzymol. *34*, 688–691.
3. Braun, J.R., Willnow, T.E., Ishibashi, S., Ashwell, G., and Herz, J. (1996). The major subunit of the asialoglycoprotein receptor is expressed on the hepatocellular surface in mice lacking the minor receptor subunit. J. Biol. Chem. *271*, 21160–21166.
4. Drickamer, K., Mamon, J.F., Binns, G., and Leung, J.O. (1984). Primary structure of the rat liver asialoglycoprotein receptor. Structural evidence for multiple polypeptide species. J. Biol. Chem. *259*, 770–778.
5. Rensen, P.C., Sliedregt, L.A., Ferns, M., Kieviet, E., van Rossenberg, S.M., van Leeuwen, S.H., van Berkel, T.J., and Biessen, E.A. (2001). Determination of the upper size limit for uptake and processing of ligands by the asialoglycoprotein receptor on hepatocytes in vitro and in vivo. J. Biol. Chem. *276*, 37577–37584.
6. Renz, M., Daniels, B.R., Vámosi, G., Arias, I.M., and Lippincott-Schwartz, J. (2012). Plasticity of the asialoglycoprotein receptor deciphered by ensemble FRET imaging and single-molecule counting PALM imaging. Proc. Natl. Acad. Sci. USA *109*, E2989–E2997.
7. Schwartz, A.L., Fridovich, S.E., and Lodish, H.F. (1982). Kinetics of internalization and recycling of the asialoglycoprotein receptor in a hepatoma cell line. J. Biol. Chem. *257*, 4230–4237.
8. Spiess, M. (1990). The asialoglycoprotein receptor: a model for endocytic transport receptors. Biochemistry *29*, 10009–10018.
9. Nair, J.K., Willoughby, J.L., Chan, A., Charisse, K., Alam, M.R., Wang, Q., Hoekstra, M., Kandasamy, P., Kel'in, A.V., Milstein, S., et al. (2014). Multivalent N-acetylgalactosamine-conjugated siRNA localizes in hepatocytes and elicits robust RNAi-mediated gene silencing. J. Am. Chem. Soc. *136*, 16958–16961.
10. Zimmermann, T.S., Karsten, V., Chan, A., Chiesa, J., Boyce, M., Bettencourt, B.R., Hutabarat, R., Nochur, S., Vaishnaw, A., and Gollob, J. (2017). Clinical proof of concept for a novel hepatocyte-targeting GalNAc-siRNA conjugate. Mol. Ther. *25*, 71–78.
11. Fitzgerald, K., Borodovsky, A., Querbes, W., et al. (2014). A subcutaneous, potent and durable RNAi platform targeting metabolic diseases, genes PCSK9, ApoC3 and ANGPLT3. Arterioscler. Thromb. Vasc. Biol. *34*, A7.
12. Fitzgerald, K., Simon, A., White, S., Borodovsky, A., Patel, N., Bettencourt, B., Clausen, V., Horton, J.D., Wijngaard, P., Kauffman, R., and Kallend, D. (2015). ALN-PCSsc, an RNAi investigational agent that inhibits PCSK9 with potential for effective quarterly or possibly bi-annual dosing: results of a single-blind, placebo-controlled, phase I single-ascending dose (SAD) and multi-dose (MD) trial in adults with elevated LDL-C, on and off statins. https://professional.heart.org/idc/groups/ahamah-public/@wcm/@sop/@scon/documents/downloadable/ucm_478898.pdf.
13. Yu, R.Z., Graham, M.J., Post, N., Riney, S., Zanardi, T., Hall, S., Burkey, J., Shemesh, C.S., Prakash, T.P., Seth, P.P., et al. (2016). Disposition and pharmacology of a GalNAc3-conjugated ASO targeting human lipoprotein (a) in mice. Mol. Ther. Nucleic Acids *5*, e317.
14. Sorensen, B., et al. (2014). A subcutaneously administered RNAi therapeutic (ALN-AT3) targeting antithrombin for treatment of hemophilia: interim Phase 1 study results in healthy volunteers and patients with hemophilia A or B. Blood *124*, 693.
15. Wittrup, A., and Lieberman, J. (2015). Knocking down disease: a progress report on siRNA therapeutics. Nat. Rev. Genet. *16*, 543–552.
16. Huang, Y. (2017). Preclinical and clinical advances of GalNAc-decorated nucleic acid therapeutics. Mol. Ther. Nucleic Acids *6*, 116–132.
17. Butler, J., et al. (2013). Aln-TMP: a subcutaneously administered RNAi therapeutic targeting TMPRSS6 for the treatment of β-thalassemia. Blood *122*, 2260.
18. Butler, J.S., Chan, A., Costelha, S., Fishman, S., Willoughby, J.L., Borland, T.D., Milstein, S., Foster, D.J., Gonçalves, P., Chen, Q., et al. (2016). Preclinical evaluation of RNAi as a treatment for transthyretin-mediated amyloidosis. Amyloid *23*, 109–118.
19. Chan, A., Liebow, A., Yasuda, M., Gan, L., Racie, T., Maier, M., Kuchimanchi, S., Foster, D., Milstein, S., Charisse, K., et al. (2015). Preclinical development of a subcutaneous ALAS1 RNAi therapeutic for treatment of hepatic porphyrias using circulating RNA quantification. Mol. Ther. Nucleic Acids *4*, e263.
20. Sehgal, A., Barros, S., Ivanciu, L., Cooley, B., Qin, J., Racie, T., Hettinger, J., Carioto, M., Jiang, Y., Brodsky, J., et al. (2015). An RNAi therapeutic targeting antithrombin to rebalance the coagulation system and promote hemostasis in hemophilia. Nat. Med. *21*, 492–497.
21. Sepp-Lorenzino, L., et al. (2015). GalNAc-siRNA conjugate ALN-HBV targets a highly conserved, pan-genotypic X-orf viral site and mediates profound and durable HBsAg silencing in vitro and in vivo. Hepatology *62*, 224A–225A.
22. Liebow, A., Li, X., Racie, T., Hettinger, J., Bettencourt, B.R., Najafian, N., Haslett, P., Fitzgerald, K., Holmes, R.P., Erbe, D., et al. (2017). An investigational RNAi therapeutic targeting glycolate oxidase reduces oxalate production in models of primary hyperoxaluria. J. Am. Soc. Nephrol. *28*, 494–503.
23. Zhang, M., Zhou, X., Wang, B., Yung, B.C., Lee, L.J., Ghoshal, K., and Lee, R.J. (2013). Lactosylated gramicidin-based lipid nanoparticles (Lac-GLN) for targeted delivery of anti-miR-155 to hepatocellular carcinoma. J. Control. Release *168*, 251–261.
24. Marshall, J.S., Green, A.M., Pensky, J., Williams, S., Zinn, A., and Carlson, D.M. (1974). Measurement of circulating desialylated glycoproteins and correlation with hepatocellular damage. J. Clin. Invest. *54*, 555–562.
25. Marshall, J.S., and Williams, S. (1978). Serum inhibitors of desialylated glycoprotein binding to hepatocyte membranes. Biochim. Biophys. Acta *543*, 41–52.
26. Marshall, J.S., Williams, S., Jones, P., and Hepner, G.W. (1978). Serum desialylated glycoproteins in patients with hepatobiliary dysfunction. J. Lab. Clin. Med. *92*, 30–37.
27. Sugahara, K., Togashi, H., Takahashi, K., Onodera, Y., Sanjo, M., Misawa, K., Suzuki, A., Adachi, T., Ito, J., Okumoto, K., et al. (2003). Separate analysis of asialoglycoprotein receptors in the right and left hepatic lobes using Tc-GSA SPECT. Hepatology *38*, 1401–1409.

28. Trerè, D., Fiume, L., De Giorgi, L.B., Di Stefano, G., Migaldi, M., and Derenzini, M. (1999). The asialoglycoprotein receptor in human hepatocellular carcinomas: its expression on proliferating cells. Br. J. Cancer *81*, 404–408.

29. Ishibashi, S., Hammer, R.E., and Herz, J. (1994). Asialoglycoprotein receptor deficiency in mice lacking the minor receptor subunit. J. Biol. Chem. *269*, 27803–27806.

30. Dalton, S.R., Wiegert, R.L., Baldwin, C.R., Kassel, K.M., and Casey, C.A. (2003). Impaired receptor-mediated endocytosis by the asialoglycoprotein receptor in ethanol-fed mice: implications for studying the role of this receptor in alcoholic apoptosis. Biochem. Pharmacol. *65*, 535–543.

31. Tworek, B.L., Tuma, D.J., and Casey, C.A. (1996). Decreased binding of asialoglycoproteins to hepatocytes from ethanol-fed rats. Consequence of both impaired synthesis and inactivation of the asialoglycoprotein receptor. J. Biol. Chem. *271*, 2531–2538.

32. Evarts, R.P., Marsden, E.R., and Thorgeirsson, S.S. (1985). Modulation of asialoglycoprotein receptor levels in rat liver by phenobarbital treatment. Carcinogenesis *6*, 1767–1773.

33. Witzigmann, D., Quagliata, L., Schenk, S.H., Quintavalle, C., Terracciano, L.M., and Huwyler, J. (2016). Variable asialoglycoprotein receptor 1 expression in liver disease: implications for therapeutic intervention. Hepatol. Res. *46*, 686–696.

34. Matsuzaki, S., Onda, M., Tajiri, T., and Kim, D.Y. (1997). Hepatic lobar differences in progression of chronic liver disease: correlation of asialoglycoprotein scintigraphy and hepatic functional reserve. Hepatology *25*, 828–832.

35. Reimer, P., Weissleder, R., Lee, A.S., Buettner, S., Wittenberg, J., and Brady, T.J. (1991). Asialoglycoprotein receptor function in benign liver disease: evaluation with MR imaging. Radiology *178*, 769–774.

36. Tozawa, R., Ishibashi, S., Osuga, J., Yamamoto, K., Yagyu, H., Ohashi, K., Tamura, Y., Yahagi, N., Iizuka, Y., Okazaki, H., et al. (2001). Asialoglycoprotein receptor deficiency in mice lacking the major receptor subunit. Its obligate requirement for the stable expression of oligomeric receptor. J. Biol. Chem. *276*, 12624–12628.

37. Akinc, A., Querbes, W., De, S., Qin, J., Frank-Kamenetsky, M., Jayaprakash, K.N., Jayaraman, M., Rajeev, K.G., Cantley, W.L., Dorkin, J.R., et al. (2010). Targeted delivery of RNAi therapeutics with endogenous and exogenous ligand-based mechanisms. Mol. Ther. *18*, 1357–1364.

38. Vera, D.R., Krohn, K.A., Stadalnik, R.C., and Scheibe, P.O. (1984). Tc-99m galactosyl-neoglycoalbumin: in vitro characterization of receptor-mediated binding. J. Nucl. Med. *25*, 779–787.

39. Virgolini, I., Angelberger, P., Müller, C., O'Grady, J., and Sinzinger, H. (1990). 99mTc-neoglycoalbumin (NGA)-binding to human hepatic binding protein (HBP) in vitro. Br. J. Clin. Pharmacol. *29*, 207–214.

40. Vera, D.R., Stadalnik, R.C., Trudeau, W.L., Scheibe, P.O., and Krohn, K.A. (1991). Measurement of receptor concentration and forward-binding rate constant via radiopharmacokinetic modeling of technetium-99m-galactosyl-neoglycoalbumin. J. Nucl. Med. *32*, 1169–1176.

41. Sato, H., Kato, Y., Hayasi, E., Tabata, T., Suzuki, M., Takahara, Y., and Sugiyama, Y. (2002). A novel hepatic-targeting system for therapeutic cytokines that delivers to the hepatic asialoglycoprotein receptor, but avoids receptor-mediated endocytosis. Pharm. Res. *19*, 1736–1744.

42. Severgnini, M., Sherman, J., Sehgal, A., Jayaprakash, N.K., Aubin, J., Wang, G., Zhang, L., Peng, C.G., Yucius, K., Butler, J., and Fitzgerald, K. (2012). A rapid two-step method for isolation of functional primary mouse hepatocytes: cell characterization and asialoglycoprotein receptor based assay development. Cytotechnology *64*, 187–195.

43. Kornilova, A.Y., Algayer, B., Breslin, M., and Uebele, V. (2012). Development of a fluorescence polarization binding assay for asialoglycoprotein receptor. Anal. Biochem. *425*, 43–46.

44. Carlson, J.A., Rogers, B.B., Sifers, R.N., Finegold, M.J., Clift, S.M., DeMayo, F.J., Bullock, D.W., and Woo, S.L. (1989). Accumulation of PiZ alpha 1-antitrypsin causes liver damage in transgenic mice. J. Clin. Invest. *83*, 1183–1190.

45. Mencin, A., Seki, E., Osawa, Y., Kodama, Y., De Minicis, S., Knowles, M., and Brenner, D.A. (2007). Alpha-1 antitrypsin Z protein (PiZ) increases hepatic fibrosis in a murine model of cholestasis. Hepatology *46*, 1443–1452.

46. Adams, D., Coelho, T., Conceicao, I., Waddington-Cruz, M., Schmidt, H., Buades, J., Campistol, J., Pouget, J., Berk, J., Falzone, R., et al. (2016). Phase 2 open-label extension study (OLE) of Patisiran, an investigational RNAi therapeutic for familial amyloid polyneuropathy (FAP). Neurology *86* (16 Suppl), S38.003.

47. Haase, N., et al. (2014). RNAi therapeutics targeting human angiotensinogen (hAGT) ameliorate preeclamptic sequelae in an established transgenic rodent model for preeclampsia. Hypertension *64*, A666–A666.

48. Dalton, S.R., Wiegert, R.L., and Casey, C.A. (2003). Receptor-mediated endocytosis by the asialoglycoprotein receptor: effect of ethanol administration on endosomal distribution of receptor and ligand. Liver Int. *23*, 484–491.

49. Iwaisako, K., Jiang, C., Zhang, M., Cong, M., Moore-Morris, T.J., Park, T.J., Liu, X., Xu, J., Wang, P., Paik, Y.H., et al. (2014). Origin of myofibroblasts in the fibrotic liver in mice. Proc. Natl. Acad. Sci. USA *111*, E3297–E3305.

50. Boveia, V., and Schutz-Geschwender, A. (2015). Quantitative analysis of signal transduction with in-cell western immunofluorescence assays. Methods Mol. Biol. *1314*, 115–130.

51. Van Berkel, T.J., Van Velzen, A., Kruijt, J.K., Suzuki, H., and Kodama, T. (1998). Uptake and catabolism of modified LDL in scavenger-receptor class A type I/II knock-out mice. Biochem. J. *331*, 29–35.